

CONF-8908158--3

UCRL--102966

DE90 008301

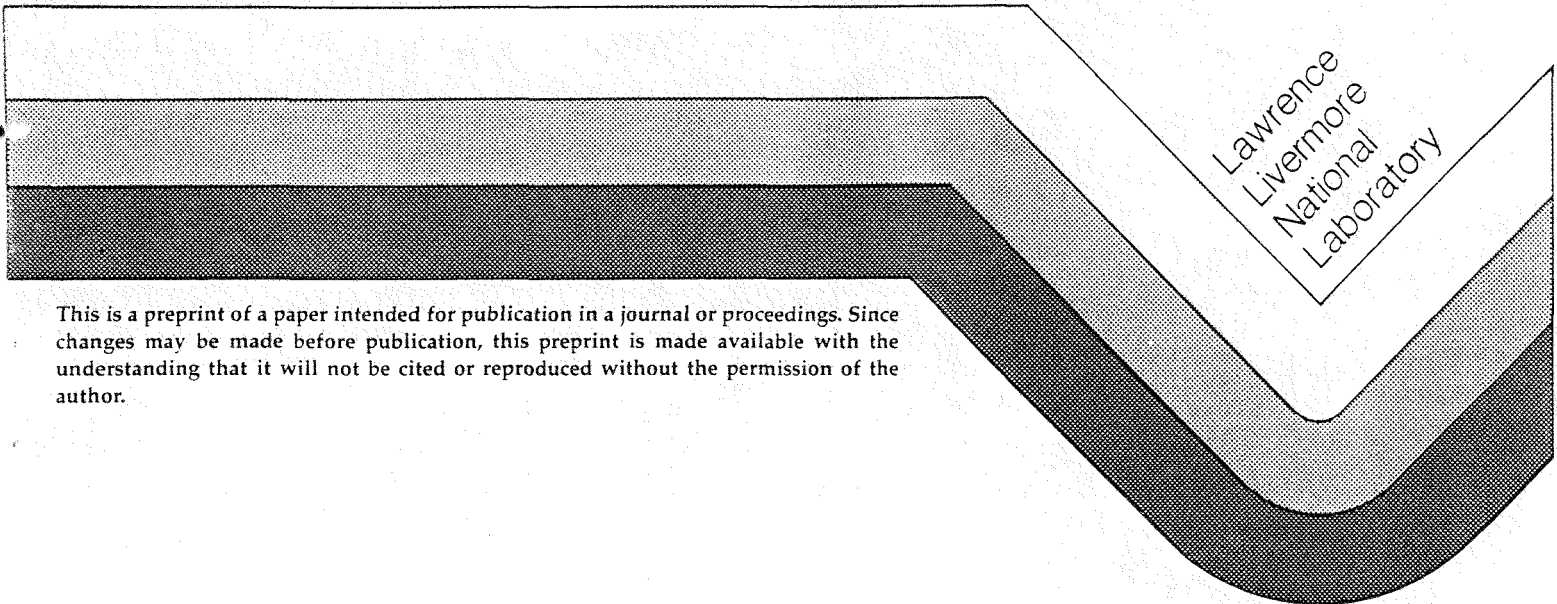
MAR 19 1990

HYDRODYNAMIC INTERACTIONS AND TRANSPORT  
COEFFICIENTS IN A SUSPENSION OF SPHERICAL PARTICLES

Anthony J. C. Ladd

This paper is to be published in  
'Microscopic Simulations of Complex Flows';  
proceedings of a meeting held at  
the Universite Libre de Bruxelles  
Bruxelles, Belgium  
August 23-25, 1989

February, 1990



This is a preprint of a paper intended for publication in a journal or proceedings. Since changes may be made before publication, this preprint is made available with the understanding that it will not be cited or reproduced without the permission of the author.

DISTRIBUTION OF THIS DOCUMENT IS UNLIMITED  
MASTER

## **DISCLAIMER**

**Portions of this document may be illegible in electronic image products. Images are produced from the best available original document.**

# HYDRODYNAMIC INTERACTIONS AND TRANSPORT COEFFICIENTS IN A SUSPENSION OF SPHERICAL PARTICLES

Anthony J.C. Ladd

Lawrence Livermore National Laboratory, Livermore, California 94550

Particulate suspensions of solids in liquids can be understood in terms of the microstructure of the solid phase by using the well-known techniques of numerical statistical mechanics. The major problem with such an approach has been the incorporation of the long-range, many-body hydrodynamic forces between the suspended particles. In this paper I describe a general computational method for calculating the forces and torques exerted by slowly moving spheres suspended in an incompressible fluid. The method can be used to determine bulk constitutive properties of solid-fluid suspensions or particulate porous media. Numerical results for the sedimentation velocity and high frequency viscosity of mono-disperse suspensions have been obtained, and the results are shown to compare very well with experimental measurement.

## 1. INTRODUCTION

Transport processes in simple liquids can be described by linear constitutive laws, characterized by transport coefficients that depend only on the thermodynamic state of the system. This is because there are large separations of length scale and time scale between the macroscopic fluxes and the underlying microscopic processes. For particulate suspensions these scale separations are not so large and the macroscopic constitutive laws can be non-local in time and non-linear in the applied fields. These complicated constitutive relations can be obtained directly from a statistical analysis of the microscopic interactions [1]. This involves first determining what the microscopic interactions are for a particular configuration of solid particles and then averaging over an appropriate ensemble of configurations to obtain macroscopic transport coefficients such as viscosity, sedimentation velocity (mobility), self-diffusion coefficients, and permeability. This is a well-defined procedure which requires as input only the distribution of solid particle sizes, the viscosity of the suspending fluid (assuming it is a simple Newtonian fluid), and a boundary condition at the solid-fluid surface, usually the hydrodynamic "no-slip" condition.

The first application of a statistical theory of particulate suspensions was contained in Einstein's thesis work around 1905. He obtained an expression, now well known, relating the viscosity of a dilute suspension of spheres  $\eta$  to the viscosity of the pure fluid  $\eta_0$  and the solid volume fraction  $\phi$  [2],

$$\eta/\eta_0 = 1 + \frac{5}{2} \phi. \quad (1.1)$$

In the dilute limit it is sufficient to treat the suspension as an assembly of non-interacting spheres, but at higher solid densities the particles interact via viscous forces transmitted through the fluid. These hydrodynamic interactions cannot be written down in closed form except in special cases: the

calculating them for arbitrary assemblies of spherical particles is the main objective of the method described in this work. Specifically, it will be assumed that the spheres are of uniform size, and that hydrodynamic stick boundary conditions apply at the solid-fluid surfaces. Then the fluid velocity field on the surface of a particle is given by

$$\mathbf{v}(\mathbf{r}) = \mathbf{U} + \boldsymbol{\Omega} \times (\mathbf{r} - \mathbf{R}) \quad \text{for } |\mathbf{r} - \mathbf{R}| = a, \quad (2.4)$$

where  $\mathbf{U}$ ,  $\boldsymbol{\Omega}$ , and  $\mathbf{R}$  are the velocity, angular velocity, and location of the particle, and  $a$  is the particle radius. Equations (2.1) and (2.4), together with periodic boundary conditions applied to a set of  $N$  spheres in a cubic unit cell of volume  $V$ , completely specify the problem, which can be solved by the method of induced forces [11].

The stick boundary conditions are satisfied by introducing an induced-force density on the surface of each particle, which is to be chosen so that the fluid velocity field matches the surface velocity of each particle [Eq. (2.4)] at all points on the particle surface. The fluid velocity field anywhere in the system can be written in terms of this induced force density  $\mathbf{F}_{\text{ind}}$ ,

$$\mathbf{v}(\mathbf{r}) = \mathbf{v}_0(\mathbf{r}) + \int_{V_M} \mathbf{T}(\mathbf{r} - \mathbf{r}') \cdot \mathbf{F}_{\text{ind}}(\mathbf{r}') d\mathbf{r}', \quad (2.5)$$

where  $\mathbf{v}_0$  is an externally imposed velocity field. The Green's function  $\mathbf{T}$  is the Oseen tensor, describing the velocity field arising from a point force in an infinite medium,

$$\mathbf{T}(\mathbf{r}) = \frac{1}{8\pi\eta_0 r} [\mathbf{I} + \hat{\mathbf{r}}\hat{\mathbf{r}}]; \quad (2.6)$$

the vector  $\hat{\mathbf{r}}$  denotes the unit vector  $\mathbf{r}/r$ , and  $\mathbf{I}$  represents the second rank unit tensor. The integral in Eq. (2.5) extends over the macroscopic sample volume  $V_M$ , and includes all the periodic images of the unit cell. Because the Oseen tensor is long-range this integral can diverge, and it is therefore necessary to take careful account of the macroscopic boundary conditions. In general there can be no net force on the fluid; otherwise it will accelerate without bound. A gravitational force, for instance, must always be balanced by a compensating pressure gradient. With this constraint, we can rewrite Eq. (2.5) in a form consistent with periodic boundary conditions [10],

$$\mathbf{v}(\mathbf{r}) = \mathbf{v}_0(\mathbf{r}) + \frac{1}{V} \sum_{\mathbf{k} \neq 0} \frac{e^{i\mathbf{k}\cdot\mathbf{r}}}{\eta_0 k^2} [\mathbf{I} - \hat{\mathbf{k}}\hat{\mathbf{k}}] \cdot \mathbf{F}_{\text{ind}}(\mathbf{k}), \quad (2.7)$$

where  $\mathbf{F}_{\text{ind}}(\mathbf{k})$  is a finite Fourier transform over the volume  $V$  of the unit cell containing the  $N$  spheres,

$$\mathbf{F}_{\text{ind}}(\mathbf{k}) = \int_V e^{-i\mathbf{k}\cdot\mathbf{r}} \mathbf{F}_{\text{ind}}(\mathbf{r}) d\mathbf{r}. \quad (2.8)$$

The sum in Eq. (2.7) includes all  $\mathbf{k}$ -vectors commensurate with the unit cell. The  $\mathbf{k} = 0$  term is omitted from the summation, as it is assumed that there is no net ( $\mathbf{k} = 0$ ) force on the system.

The periodic Oseen equation [Eq. (2.7)] can be solved by a multipole expansion of the induced force density on the surface of each particle. Force multipoles are defined as surface integrals involving the induced traction  $\mathbf{t}_i$  (*i.e.* the induced force per unit area on the particle surface) and irreducible tensor products of the unit vector  $\hat{\mathbf{r}}_i$ , which denotes a point on the surface of sphere  $i$  relative to its center [9]. Thus the  $p$ -th order force multipole of particle  $i$  is a tensor of rank  $p+1$

$$\mathbf{F}_i^{p+1} = \frac{1}{p!} \int_{S_i} \hat{\mathbf{r}}_i^p \mathbf{t}_i(\mathbf{r}_i) d\mathbf{r}_i, \quad (2.9)$$

where  $S_i$  indicates an integral over the (spherical) surface of particle  $i$ . The notation  $\hat{\mathbf{r}}^p$  is used to indicate an irreducible tensor of rank  $p$ . The forces, torques, and stress exerted by the fluid on a particular

$\zeta^{2s,2s}$ , as discussed in section 3.

When a pair of particles is close to contact the hydrodynamic forces diverge as  $s^{-1}$  and  $\ln s^{-1}$ , where  $s = (R_{12} - 2a)/a$  is the gap between the particles relative to the radius. Under these circumstances the multipole moment expansion described above converges very poorly, or not at all [10]. However, since these lubrication forces are dominated by the interactions between contact points rather than boundary surfaces, they are pairwise additive. Thus we can replace the approximate pairwise-additive friction coefficients in Eqs. (2.16) with the exact ones [7], which are already known from other work [13-15]. The computational overhead is negligible, since the two-body friction coefficients are just scalar functions of the interparticle separation multiplied by appropriate spherical harmonics to describe the angular variation. The scalar functions, computed from the difference between the exact and approximate two-particle friction coefficients, were stored in tabular form at 1000 points between  $R = 2a$  and  $R = 4a$ . The interpolation procedure used ensures that the  $s^{-1}$  and  $\ln s^{-1}$  singularities are handled exactly.

### 3. TRANSPORT COEFFICIENTS

The transport properties of a random dispersion of hard spheres have been a subject of theoretical investigation for a long time [1]. In this paper we consider only the sedimentation velocity (mobility) and the high-frequency viscosity; other transport coefficients are considered elsewhere [12]. An underlying assumption is that the distribution of configurations of spheres is the equilibrium one, unaffected by the hydrodynamic interactions. This assumption is strictly valid only at short times or high frequencies.

The transport coefficients we are interested in are related to ensemble averages of the appropriate elements of the friction and mobility tensors. The collective mobility (sedimentation velocity) is obtained from the velocity response of the  $N$ -particle suspension to an applied force, and thus from Eq. (2.3a)

$$\mu = N^{-1} \frac{1}{3} \text{tr} \left\langle \sum_{i,j=1}^N \mu_{ij}^{\text{TT}} \right\rangle, \quad (3.1)$$

where

$$\begin{bmatrix} \mu^{\text{TT}} & \mu^{\text{TR}} \\ \mu^{\text{RT}} & \mu^{\text{RR}} \end{bmatrix} = \begin{bmatrix} \zeta^{\text{TT}} & \zeta^{\text{TR}} \\ \zeta^{\text{RT}} & \zeta^{\text{RR}} \end{bmatrix}^{-1}. \quad (3.2)$$

Our results are expressed in terms of the dimensionless quantity  $\mu/\mu_0$ , where  $\mu_0 = (6\pi\eta_0 a)^{-1}$  is the mobility of an isolated sphere of radius  $a$ .

In section II it was shown how to calculate the dissipative hydrodynamic forces acting on suspended particles that are moving under the influence of external forces or fluctuating Brownian forces. We are also interested in the response of the suspension to a homogeneous external shear rate. In this work we will ignore the effects of the imposed flow on the suspension microstructure and assume that it is an equilibrium distribution of hard spheres, freely moving with the flow without hydrodynamic forces and torques. Such a situation can be realized experimentally by using an oscillating strain rate with a sufficiently high frequency that the solid particles cannot follow the imposed fluid flow. The theory developed in Ref. [9], summarized here, applies to that situation: low frequency transport coefficients will be considered in future work.

The stress in a suspension subjected to a homogeneous external shear rate  $\dot{\epsilon}_0^s$  contains a contribution from the velocity gradients in the fluid and a contribution from the forces exerted by the fluid on the solid-particle surfaces. This latter contribution is related to the external shear rate by the ensemble-averaged dipole-dipole friction tensor [Eqs. (2.10), (2.12), and (2.14)]

$$\langle \zeta^{2s,2s} \rangle = N^{-1} \left\langle \sum_{i,j=1}^N \zeta_{ij}^{2s,2s} \right\rangle \quad (3.3)$$

Table 1. Dependence of the mobility ( $\mu$ ) and viscosity ( $\eta$ ) on the number of force moments.

$\phi$	$N$	$p_{\max}$	$\mu/\mu_0$	$\eta/\eta_0$
0.45	16	1	0.0982(5)	5.41(4)
		2	0.0480(3)	5.29(4)
		3	0.0439(2)	5.48(4)
		4	0.0418(2)	5.41(4)
		5	0.0415(2)	5.54(5)
		6	0.0412(2)	5.55(5)
		7	0.0410(2)	5.50(4)
	32	1	0.1012(2)	5.70(2)
		2	0.0499(2)	5.53(2)
		3	0.0453(1)	5.58(2)
		4	0.0433(2)	5.63(2)
		5	0.0427(1)	5.65(2)
	54	1	0.1014(2)	5.69(2)
		2	0.0505(1)	5.55(2)
		3	0.0460(1)	5.61(2)
	108	1	0.1018(2)	5.73(1)
		2	0.0507(2)	5.52(2)

It is not computationally feasible at present to run the larger systems with the same number of force moments as the 16-particle systems; we used force moments up to  $p_{\max} = 5$ ,  $p_{\max} = 3$ , and  $p_{\max} = 2$  for the  $N = 32$ ,  $N = 54$ , and  $N = 108$  particle systems respectively. Fortunately the higher force moments are only important for clusters of particles that are relatively close together, and therefore their effects are more or less independent of system size. This can be verified from Table 1 by noting that the difference between mobility coefficients derived from successive moment approximations is essentially independent of  $N$ . Thus we can estimate the large  $p_{\max}$  results for all the system sizes considered, assuming the effects of the higher force moments are the same as for  $N = 16$ . This leads to consistent results for the  $p_{\max} \rightarrow \infty$  mobility coefficients even at  $\phi = 0.45$  where the high-moment effects are most important. The fully converged transport coefficients for the different size systems, over a range of packing fractions, are shown in Table 2.

Table 2. Variation of the mobility ( $\mu$ ) and viscosity ( $\eta$ ) with system size. Finite-size corrections for the mobility coefficient are shown in parentheses, followed by the resulting estimate for  $N \rightarrow \infty$ .

$\phi$	$N$	$\mu/\mu_0$	$\eta/\eta_0$
0.01	16	0.800 (+ 0.137 = 0.937)	1.02547
	32	0.829 (+ 0.109 = 0.938)	1.02550
	54	0.839 (+ 0.091 = 0.930)	1.02549
	108	0.868 (+ 0.073 = 0.941)	1.02549
0.05	16	0.570 (+ 0.164 = 0.734)	1.1383
	32	0.600 (+ 0.130 = 0.730)	1.1387
	54	0.621 (+ 0.109 = 0.730)	1.1389
	108	0.640 (+ 0.087 = 0.727)	1.1391
0.25	16	0.162 (+ 0.039 = 0.201)	2.17
	32	0.167 (+ 0.031 = 0.198)	2.17
	54	0.174 (+ 0.027 = 0.201)	2.17
	108	0.178 (+ 0.021 = 0.199)	2.17
0.45	16	0.0410 (+ 0.0041 = 0.0451)	5.5
	32	0.0423 (+ 0.0034 = 0.0457)	5.6
	54	0.0431 (+ 0.0029 = 0.0460)	5.6
	108	0.0437 (+ 0.0023 = 0.0460)	5.6

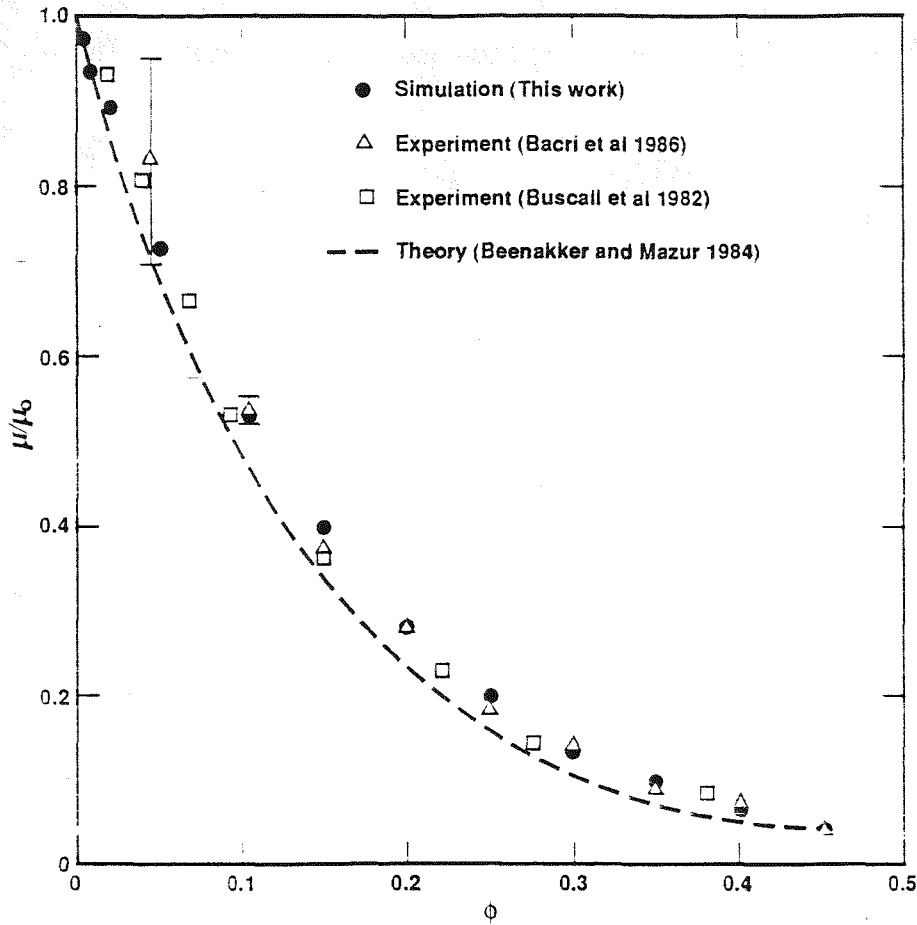


Figure 1. Short-time sedimentation velocity (mobility) of suspended hard spheres. The solid circles are the simulation results; the open symbols are experimental results from Buscall et. al. [20], and Bacri et. al. [21]. The dashed line is the theoretical analysis of Beenakker and Mazur [23].

The dashed lines in Figs. 1 and 2 are theoretical results of Beenakker and Mazur [23,25], based on calculating the hydrodynamic interactions in an effective medium that includes average many-body contributions. The theoretical results are in good agreement overall with the simulations: the worst discrepancy, around  $\phi = 0.25$  in the collective mobility, is still only about 20%. The simulation results do not support recent speculation that the collective mobility coefficient of a random dispersion of hard spheres vanishes at a relatively low packing fraction ( $\phi \approx 0.15$ ) [26].

The high-frequency viscosity is shown in Fig. 2. The experimental results of Van der Werff et. al. [27] were derived from oscillating Couette viscometry. The results shown here correspond to a sufficiently high frequency that the solid particles are unaffected by the imposed shear flow, so that the distribution of configurations is just the equilibrium distribution assumed in the simulations. At the lower packing fractions ( $\phi < 0.35$ ) the experimental and simulation results are indistinguishable, but at high packing fractions there is some spread in the experimental data depending on the particle size. The larger size particles tend to have the larger viscosities, which are in better agreement with our simulations than the results for smaller spheres.

An expression for the viscosity has been proposed by Bedeaux [28]

$$\frac{\eta/\eta_0 - 1}{\eta/\eta_0 + 3/2} = \phi[1 + S(\phi)], \quad (3.12)$$

which incorporates a mean-field description of the hydrodynamic interactions when  $S(\phi) = 0$ . Thus a virial expansion of  $S(\phi)$  should lead to a more rapidly converging viscosity than the usual expansion of  $\eta/\eta_0$ . Van der Werff et. al. [27] used their experimental data to deduce an expansion for  $S$ .

$$S(\phi) = (1.41 \pm 0.14)\phi - (1.19 \pm 0.34)\phi^2; \quad (3.13)$$

Thus systems of several hundred particles would fit in the core memory of a modern supercomputer. A further constraint is that the triangular decomposition of the  $G$  matrix requires of the order of  $(Np_{\max}^2)^3$  operations; but by using an iterative method, such as conjugate directions, the simultaneous equations [Eqs. (2.14)] can be solved in a time of order  $(Np_{\max}^2)^2$ , for a specified set of velocities or forces. Thus for high Peclet-number flows, where Brownian motion can be ignored, it should be possible to simulate systems of about one hundred particles at high packing fractions ( $p_{\max} = 6$  or  $7$ ) and several hundred particles at lower packing fractions. However, to include random displacements (or velocities) all the elements of the  $6N \times 6N$  mobility (or friction coefficient) matrix must be computed, which inevitably requires of the order of  $N^3$  operations [30].

An interesting alternative to integral-equation methods is the use of lattice-gas cellular automata to model the fluid phase [31]. Lattice-gas models are simplified molecular models in which particles with a discrete set of velocities move from one node to another of a space-filling lattice, undergoing collisions with other particles occupying the same nodes. For a sufficiently large number of particles these models are equivalent to the continuum Navier-Stokes equations [32], with the very significant advantage that thermal fluctuations, which give rise to Brownian motion, are also included [31]. Moreover the computational requirements scale as  $N$  instead of  $N^2$  or  $N^3$  as is the case for the integral equation methods. Recent studies of the hydrodynamic interactions between moving spheres [33] have shown that there is quantitative agreement between the results of lattice-gas simulations and lubrication theory down to gaps of the order of a lattice spacing. The combination of particle models of the solid phase and lattice-gas models of the fluid phase can handle the whole range of solid-fluid suspensions, from sub-micron particle sizes where Brownian motion is important, to macroscopic size particles.

In the future both the creeping-flow and lattice-gas models of the fluid phase will be used to study the rheological properties of suspensions by computer simulation. These simulations will incorporate the dynamical effects of the hydrodynamic forces on the structure of the suspension [30], which are crucial to quantitative predictions of low-frequency suspension rheology [34].

#### ACKNOWLEDGEMENTS

I would like to thank Prof. John Brady (CalTech) for providing a complete list of asymptotic expansions for the lubrication forces. I would also like to thank Prof. S. Kim (University of Wisconsin) for providing a copy of the computer program, written by himself and Dr. R. Mifflin (Princeton University), to calculate hydrodynamic interactions between pairs of particles. This work was supported by the U.S. Department of Energy and Lawrence Livermore National Laboratory under Contract No. W-7405-Eng-48.

#### REFERENCES

- [1] J. Happel and H. Brenner, *Low-Reynolds Number Hydrodynamics*, (Martinus Nijhoff, Dordrecht, 1986).
- [2] A. Einstein, *Investigations on the Theory of the Brownian Movement*, (Dover Publications, New York, 1956).
- [3] D.L. Ermak and J.A. McCammon, *J. Chem. Phys.* **69**, 1352 (1978).
- [4] W. Van Meegen and I. Snook, *J. Chem. Soc. Farad. Trans. II.* **80**, 383 (1984).
- [5] J.F. Brady and G. Bossis, *J. Fluid Mech.* **155**, 105 (1985).
- [6] C.W.J. Beenakker and P. Mazur, *Physica A* **120**, 388 (1983).
- [7] L. Durlofsky, J.F. Brady and G. Bossis, *J. Fluid Mech.* **180**, 21 (1987).
- [8] R.J. Phillips, J.F. Brady and G. Bossis, *Phys. Fluids* **31**, 3462 (1988).
- [9] A.J.C. Ladd, *J. Chem. Phys.* **88**, 5051 (1988).
- [10] A.J.C. Ladd, *J. Chem. Phys.* **90**, 1149 (1989).
- [11] P. Mazur and W. Van Saarloos, *Physica A* **115**, 21 (1982).
- [12] A.J.C. Ladd, *J. Chem. Phys.* submitted (1989).
- [13] D.J. Jeffrey and Y. Onishi, *J. Fluid Mech.* **139**, 261 (1984).
- [14] S. Kim and R.T. Mifflin, *Phys. Fluids* **28**, 2033 (1985).
- [15] D.J. Jeffrey and R.M. Corless, *PhysicoChem. Hydrodyn.* **10**, 461 (1988).
- [16] B.U. Felderhof, *Physica A* **82**, 611 (1976).
- [17] B.U. Felderhof, *Physica A* **159**, 1 (1989).
- [18] R.L. Triclar and A.J. Masters, *Mol. Phys.* **67**, 1273 (1989).